Journal of Computational and Applied Mathematics 230 (2009) 8–21

Contents lists available at ScienceDirect

Journal of Computational and Applied Mathematics

journal homepage: www.elsevier.com/locate/cam

Numerical simulation of blowup in nonlocal reaction–diffusion equations using a moving mesh method[☆]

Jingtang Ma[a], Yingjun Jiang[b,*], Kaili Xiang[a]

[a] School of Economic Mathematics, South-Western University of Finance and Economics, Chengdu, 610074, China

[b] Department of Mathematics and Scientific Computing, Changsha University of Science and Technology, Changsha, 410076, China

ARTICLE INFO

Article history:
Received 13 July 2008
Received in revised form 23 October 2008

MSC:
65R20
65N50
65M50
35K55
35K57
65N35

Keywords:
Blowup
Nonlocal reaction–diffusion equations
Integro-differential equations
Moving mesh methods

ABSTRACT

In this paper we implement the moving mesh PDE method for simulating the blowup in reaction–diffusion equations with temporal and spacial nonlinear nonlocal terms. By a time-dependent transformation, the physical equation is written into a Lagrangian form with respect to the computational variables. The time-dependent transformation function satisfies a parabolic partial differential equation — usually called moving mesh PDE (MMPDE). The transformed physical equation and MMPDE are solved alternately by central finite difference method combined with a backward time-stepping scheme. The integration time steps are chosen to be adaptive to the blowup solution by employing a simple and efficient approach. The monitor function in MMPDEs plays a key role in the performance of the moving mesh PDE method. The dominance of equidistribution is utilized to select the monitor functions and a formal analysis is performed to check the principle. A variety of numerical examples show that the blowup profiles can be expressed correctly in the computational coordinates and the blowup rates are determined by the tests.

1. Introduction

Moving mesh methods have been proved to be very efficient in resolving singular solutions to reaction–diffusion equations. We are interested in implementing the moving methods to solving blow-up reaction–diffusion equations with nonlocal nonlinear terms.

In particular, we consider problems with nonlocal reaction terms in time:

$$u_t - u_{xx} = f\left(u(x,t), \int_0^t g(x,t,s,u(x,s))\,\mathrm{d}s\right), \quad t > 0, x \in \Omega \subset \mathbb{R}, \tag{1}$$

with homogeneous boundary condition $u|_{\partial\Omega} = 0$ and initial condition $u(x,0) = u_0(x)$. This type of equation is also called Volterra integro-differential equation which arises in many applications [9]. This equation is usually regarded as the mid-state between parabolic and hyperbolic equations (see cf. [8,14]). This equation (with weakly singular kernel and neutral terms) also closely relates to the time fractional differential equations, where the fractional derivatives are given by either the Riemann–Liouville derivative

$$D_t^\beta u(x,t) = \frac{1}{\Gamma(m-\beta)} \frac{\partial^m}{\partial t^m} \int_0^t (t-\tau)^{m-\beta-1} u(x,\tau)\,\mathrm{d}\tau, \quad \beta \in (m-1, m),$$

or the Caputo derivative

☆ The research was supported by SRF for ROCS, SEM.

* Corresponding author.
E-mail addresses: mjt@swufe.edu.cn (J. Ma), jiangyingjun@csust.edu.cn (Y. Jiang), xiangkl@swufe.edu.cn (K. Xiang).

0377-0427/$ – see front matter © 2008 Elsevier B.V. All rights reserved.
doi:10.1016/j.cam.2008.10.063

$$D_t^\beta u(x,t) = \frac{1}{\Gamma(m-\beta)} \int_0^t (t-\tau)^{m-\beta-1} \frac{\partial^m u(x,\tau)}{\partial \tau^m}\, d\tau, \quad \beta \in (m-1, m),$$

where $m \in \mathbb{Z}^+$ (see e.g., in [11,12]). Part of the blowup theory for the time fractional ordinary differential equations is investigated in [23], while, to the best our knowledge, the blowup theory for the time fractional partial differential equations is completely unknown. The numerical simulation (using moving mesh methods) will be an interesting and challenging topic. In this paper we only simulate the blowup with the theories given by e.g., [28,26,19,15,3,22].

In addition, we study problems with nonlocal reaction terms in space:

$$u_t - u_{xx} = f\left(u(x,t), \int_\Omega g(t, u(y,t))\, dy\right), \quad t > 0, x \in \Omega \subset \mathbb{R}, \tag{2}$$

with $u|_{\partial\Omega} = 0$ and $u(x,0) = u_0(x)$. The readers are referred to e.g., [6,29,27,28,1,13,2] and the references therein for the mathematical theory of blowup.

As shown in the blowup theories, with sufficiently large initial data and other particular assumptions, the solutions of problems (1) and (2) will become infinite as $t \to T$ at one or several spatial locations. This phenomenon is called finite time blowup. The counter PDE (without nonlocal terms) with blowup has been understood thoroughly due to the findings of self-similar properties. In general such self-similarity in blow-up equations with nonlocal terms has not yet been found. Hence it becomes much challenging to develop the blowup theory and perform effective numerical simulations.

In this paper, we study the moving mesh PDE (MMPDE) methods, which are widely admitted to be successful in solving blowup problems (see e.g., [7,5,24,25,16]), for simulation of the blowup in nonlocal reaction–diffusion equations — (1) and (2). To be more precise, define a time-dependent transformation $x(\xi, t)$ from computational coordinate ξ to physical coordinate x such that it satisfies a parabolic PDE — MMPDE6 (see e.g., [17]):

$$-\tau \frac{\partial^2 \dot{x}}{\partial \xi^2} = \frac{\partial}{\partial \xi}\left(M \frac{\partial x}{\partial \xi}\right), \tag{3}$$

with $x(0,t)$ and $x(1,t)$ being the left and right boundaries of Ω, respectively, where $M = M(x,t)$ is the monitor function that depends on the physical solution and used for controlling mesh concentration, and $\tau > 0$ is a parameter used for adjusting the response time of mesh movement to changes in M. The idea of moving mesh method originates from the equidistribution principle (see e.g., in [10]). The continuous form of equidistribution principle is employed in [17]:

$$0 = \frac{\partial}{\partial \xi}\left(M \frac{\partial x}{\partial \xi}\right).$$

Unfortunately this equidistribution principle cannot be realized in practice. Huang et al. [17] add a stabilization term $-\tau \frac{\partial^2 \dot{x}}{\partial \xi^2}$ to the left-hand-side term of the above equation, then it becomes MMPDE6. The authors [17] also derive other six labeled MMPDEs in a similar manner.

Using the transformation $x(\xi, t)$, we recast Eqs. (1) and (2) into a Lagrangian form

$$\dot{(x_\xi u)} - (\dot{x}_\xi u + \dot{x} u_\xi) - \left(\frac{u_\xi}{x_\xi}\right)_\xi = x_\xi (\text{nonlocal term}), \tag{4}$$

where the right-hand side corresponds to the nonlocal reaction terms with replacement of x by $x(\xi, t)$. The solution u in computational coordinate ξ is smooth and thus can be efficiently solved using uniform meshes. Combining the transformed equation with the MMPDE6 forms a highly coupled nonlinear system for unknown functions u and x. The two equations in the system are solved alternately by finite difference methods for computational coordinates ξ and time t. Paper [18] analyzes this moving mesh method for the problems with linear nonlocal reaction terms and proves second-order convergence in space and first-order convergence in time.

Now we are in a position to discuss the monitor function M in the MMPDE6. We consider monitor functions of the general forms

$$M(x,t) = u^\gamma, \quad \text{for which the reaction term is the functional of } u^p \tag{5}$$

or

$$M(x,t) = (\exp(u))^\gamma, \quad \text{for which the reaction term is the functional of } \exp(u), \tag{6}$$

where $\gamma > 0$ is a parameter. The key to MMPDE method is to determine the monitor function, that is, decide the value of the constant γ. Paper [7] uses scaling invariance of the MMPDE with sufficiently small time instance τ, consistent with a similar property of the physical PDEs (without nonlocal terms), to determine the value of γ. However the approach for PDEs is not applicable to the nonlocal equations, since the scaling invariance is not known. Recently paper [16] proves that the scaling invariance is neither necessary nor sufficient to simulate blowup in reaction–diffusion equations. Instead, the dominance of equidistribution is not only sufficient but also necessary condition for constant τ. The dominance of equidistribution means that the asymptotic behavior of $\frac{\partial}{\partial \xi}\left(M \frac{\partial x}{\partial \xi}\right)$ dominates the other terms in MMPDE as $t \to T$. In this paper, we will use the dominance of equidistribution to determine the value of γ in the monitor functions. In the process, a formal analysis — dimensional analysis (see e.g., [4]) is used to examine the dominance of equidistribution.

In the following Sections 2 and 3, we study the problems with nonlocal terms in time and in space as well. We give the additional comments and conclusions in the final section.

2. Problems with nonlocal reaction terms in time

2.1. Dimensional analysis and monitor functions

In this section we study three particular examples for equations with temporal nonlocal terms (1).

One example is

$$u_t - u_{xx} = \int_0^t u^p(x,s)\,\mathrm{d}s, \quad t > 0, x \in \Omega \subset \mathbb{R}, \tag{7}$$

with boundary and initial conditions: $u|_{\partial\Omega} = 0, u(x,0) = u_0(x)$. The blowup theory for this equation is first studied in [26]: if $p > 1$ and the initial function $u_0 \ge 0$, then the solution has finite time blowup. Later in [28] (compare also [20]) the authors prove the blowup rate:

$$\max_{x\in\overline{\Omega}} u(x,t) \approx (T-t)^{-2/(p-1)}, \quad \text{as } t \to T, \tag{8}$$

if the initial function has the form: $u_0 = \lambda\Phi$, with sufficiently large positive constant λ and with positive function Φ satisfying that $\Phi \in C^2(\Omega), \Phi|_{\partial\Omega} = 0$; moreover there exists $\epsilon, \sigma > 0$ such that

$$\Phi_{xx} \ge \epsilon \,\mathrm{dist}(x, \partial\Omega), \quad \text{for all } x \in \Omega \text{ such that } \mathrm{dist}(x,\partial\Omega) \le \sigma.$$

In the following we will perform the dimensional analysis on the physical equation and MMPDE6. Following paper [16], we denote the dimensions of variables u, t, and x by $[u]$, $[t]$, and $[x]$, respectively. Then, the dimensions of the terms u_t, u_{xx}, and $\int_0^t u^p(x,s)\,\mathrm{d}s$ in the equation are given by

$$[u_t] = \frac{[u]}{[t]}, \qquad [u_{xx}] = \frac{[u]}{[x]^2}, \qquad \left[\int_0^t u^p(x,s)\,\mathrm{d}s\right] = [t][u]^p.$$

The fact that all terms in the physical PDE are dimensionally homogeneous implies that

$$\frac{[u]}{[t]} = \frac{[u]}{[x]^2} = [t][u]^p.$$

Let $\beta = 1/(p-1)$. Then this gives the dimension relations

$$[x] = [t]^{\frac{1}{2}}, \qquad [u] = [t]^{-\frac{2}{p-1}} = [t]^{-2\beta}. \tag{9}$$

We now analyze the dimensions of MMPDE6. The dimensional equation for MMPDE6 is

$$\frac{[\tau]\,[x]}{[t]} = [M][x],$$

or after simplification,

$$\frac{[\tau]}{[t]} = [M]. \tag{10}$$

For the monitor function in the form (5), the equation becomes

$$\frac{[\tau]}{[t]} = [u]^\gamma, \tag{11}$$

and using (9),

$$[\tau]\,[t]^{2\beta\gamma-1} = 1. \tag{12}$$

This indicates that the magnitude of the left-hand-side term of MMPDE6 in (3) is of order $[\tau]\,[t]^{2\beta\gamma-1}$ compared to that of the right-hand-side term. For the situation where τ is taken as constant, we have $[\tau] = 1$. In addition, for problem (7), the time scale can be taken as $[t] = T - t$ (see e.g., [28]), which becomes increasingly small as $t \to T$. Then from (12) we can see that the left-hand-side term is vanishing as $t \to T$ when $2\beta\gamma > 1$. In this case, the equidistribution term dominates and thus MMPDE6 has the dominance of equidistribution. The critical case is $2\beta\gamma = 1$, in which case the dominance of equidistribution happens only when τ is sufficiently small.

The second example we consider is

$$u_t - u_{xx} = \int_0^t u^p(x,s)\,\mathrm{d}s - u^q, \quad t > 0, x \in \Omega \subset \mathbb{R}, \tag{13}$$

with initial function $u(x,0) = u_0$ and zero boundary conditions. The blowup theory for this equation is studied in [26]: Assume that $p > q \ge 1$, and $u_0 \in C^1(\Omega), u_0 \ge 0, u_0|_{\partial\Omega} = 0$. Then the solution blows up in finite time.

After performing a similar dimensional analysis, we conclude that the dimension is balanced for the case $p = 2q - 1$. In this case, for the monitor function of the form (5), it requires that $2\beta\gamma \ge 1$. For the case $p \ne 2q - 1$, let $v + w = u$. Then

Table 1
Monitor functions $M = u^\gamma$ for Eqs. (7), (13) and (16).

Eq. (7) with $p > 1$	Eq. (13) with $p > q \geq 1$		Eq. (16) with $p, q \geq 1$
$\gamma \geq \frac{p-1}{2}$	$\gamma \geq \frac{p-1}{2}$ $\gamma \geq \max\left\{\frac{p-1}{2}, q-1\right\}$	if $p = 2q-1$; if $p \neq 2q-1$	$\gamma \geq \frac{p+q-1}{2}$

we can split Eq. (13) into two equations:

$$v_t - v_{xx} = \int_0^t u^p(x,s)\,ds; \tag{14}$$

$$w_t - w_{xx} = -u^q. \tag{15}$$

Note that $[v] = [w] = [u]$. Then for (14) and (15), the dimensional equations are given respectively by

$$\frac{[u]}{[t]} = \frac{[u]}{[x]^2} = [t][u]^p,$$

and

$$\frac{[u]}{[t]} = \frac{[u]}{[x]^2} = [u]^q.$$

Therefore, combining the dimensional Eq. (11) for MMPDE6, we obtain a sufficient condition for dominance of equidistribution, $2\beta\gamma \geq 1$ and $\eta\gamma \geq 1$, $\eta = 1/(q-1)$ (when equalities hold, τ has to be sufficiently small to keep the dominance of equidistribution). Hence for Eq. (13), it requires that $\gamma \geq \max\{1/(2\beta), 1/\eta\}$ to guarantee the dominance of equidistribution.

The last example in this section is

$$u_t - u_{xx} = \left(\int_0^t u^p(x,s)\,ds\right) u^q(x,t), \quad t > 0, x \in \Omega \subset \mathbb{R}, \tag{16}$$

subject to the same initial and boundary conditions as the above examples. The finite time blowup theory is given in [15] for $p, q \geq 1$ and for sufficiently large initial data.

The dimensional analysis gives that

$$\frac{[u]}{[t]} = \frac{[u]}{[x]^2} = [t][u]^{p+q}.$$

Therefore combining with the dimensional analysis of MMPDE6, we obtain $2\gamma/(p+q-1) > 1$ to guarantee dominance of equidistribution, and for the critical situation $2\gamma/(p+q-1) = 1$, τ has to be sufficiently small.

We summarize the above results in Table 1.

2.2. Numerical experiments

Let $\Omega = (0,1)$. We give the numerical results for examples (7) and (13) with initial conditions $u_0 = 20\sin(\pi x)$, and (16) with $u_0 = 100\sin(\pi x)$. Let N be the number of spatial mesh points and

$$0 = t_0 < t_1 < \cdots < t_{n-1} < t_n < \cdots$$

be the time mesh. Moreover denote $\Delta t_n = t_{n+1} - t_n$. In the tests for (7) and (13), we take $N = 81$, and for (16), $N = 101$. Introduce notations

$$x_j^n = x(\xi_j, t_n), \qquad u_j^n \approx u(x_j^n, t_n).$$

Then we describe the solution process in the following algorithm.

Algorithm 1. Given that the solution and mesh at t_k level – $\{u_j^k, x_j^k\}$, $k = 0, 1, \ldots, n$, we compute the solution and mesh at t_{n+1} level – $\{u_j^{n+1}, x_j^{n+1}\}$ by the following steps.

Step 1: Solve the physical Eq. (1) at the **fixed mesh** $\{x_j^n\}$ over $[t_n, t_{n+1}]$ by

$$\begin{aligned}\frac{\widetilde{u}_j^{n+1} - \widetilde{u}_j^n}{\Delta t_n} &= \frac{2}{x_{j+1}^n - x_{j-1}^n}\left[\frac{\widetilde{u}_{j+1}^{n+1} - \widetilde{u}_j^{n+1}}{x_{j+1}^n - x_j^n} - \frac{\widetilde{u}_j^{n+1} - \widetilde{u}_{j-1}^{n+1}}{x_j^n - x_{j-1}^n}\right] \\ &\quad + f\left(\widetilde{u}_j^{n+1}, \sum_{k=0}^n \Delta t_k \frac{g\left(x_j^n, t_{n+1}, t_k, \sum_{j=1}^N \widetilde{u}_j^k \phi_j^k(x_j^n)\right) + g\left(x_j^n, t_{n+1}, t_{k+1}, \sum_{j=1}^N \widetilde{u}_j^{k+1}\phi_j^{k+1}(x_j^n)\right)}{2}\right)\end{aligned} \tag{17}$$

with $\widetilde{u}_j^k = u_j^k$, $k = 0, 1, \ldots, n$, where $\phi_j^k(x)(j = 1, \ldots, N)$ are the piecewise linear nodal basis functions based on the points x_j^k, for $j = 1, \ldots, N$.

Step 2: Solve the MMPDE6 (3) by

$$\begin{aligned}&-\tau\frac{(x_{j+1}^{n+1} - 2x_j^{n+1} + x_{j-1}^{n+1}) - (x_{j+1}^n - 2x_j^n + x_{j-1}^n)}{\Delta t_n}\\ &\quad = \frac{M(\widetilde{u}_j^{n+1}) + M(\widetilde{u}_{j+1}^{n+1})}{2}(x_{j+1}^{n+1} - x_j^{n+1}) - \frac{M(\widetilde{u}_{j-1}^{n+1}) + M(\widetilde{u}_j^{n+1})}{2}(x_j^{n+1} - x_{j-1}^{n+1}). \end{aligned}\tag{18}$$

Step 3: Solve the transformed Eq. (4) by

$$\begin{aligned}&\frac{(x_{j+1}^{n+1} - x_{j-1}^{n+1})u_j^{n+1} - (x_{j+1}^n - x_{j-1}^n)u_j^n}{\Delta t_n} = 2\left[\frac{u_{j+1}^{n+1} - u_j^{n+1}}{x_{j+1}^{n+1} - x_j^{n+1}} - \frac{u_j^{n+1} - u_{j-1}^{n+1}}{x_j^{n+1} - x_{j-1}^{n+1}}\right]\\ &\quad + \left[\frac{x_{j+1}^{n+1} - x_{j+1}^n}{\Delta t_n} - \frac{x_{j-1}^{n+1} - x_{j-1}^n}{\Delta t_n}\right]u_j^{n+1} + \frac{x_j^{n+1} - x_j^n}{\Delta t_n}(u_{j+1}^{n+1} - u_{j-1}^{n+1}) + (x_{j+1}^{n+1} - x_{j-1}^{n+1})\\ &\quad \times f\left(u_j^{n+1}, \sum_{k=0}^{n}\Delta t_k \frac{g\left(x_j^{n+1}, t_{n+1}, t_k, \sum_{j=1}^{N} u_j^k\phi_j^k(x_j^{n+1})\right) + g\left(x_j^{n+1}, t_{n+1}, t_{k+1}, \sum_{j=1}^{N} u_j^{k+1}\phi_j^{k+1}(x_j^{n+1})\right)}{2}\right). \end{aligned}\tag{19}$$

During the solution process, we choose the integration time step $\Delta t_n = t_{n+1} - t_n$ as

$$\Delta t_n = \frac{\mathrm{d}t}{[\max_{(j)}\{u_j^n\}]^{\gamma'}},\tag{20}$$

where dt is a small positive constant, γ' is a positive constant.

We take problem (7) as an example to illustrate the efficiency of the method for choosing the time steps. Let

$$\gamma' = \frac{1}{2\beta} + \kappa, \quad \text{with } 0 \le \kappa \le 1.$$

Then using (8) we obtain that

$$\Delta t_n = \frac{\mathrm{d}t}{[\max_{(j)}\{u_j^n\}]^{\gamma'}} \approx \frac{\mathrm{d}t}{[\max_{\overline{\Omega}}\{u(x, t_n)\}]^{\gamma'}} \approx \frac{\mathrm{d}t}{[\max_{\overline{\Omega}}\{u(x, t_n)\}]^{\kappa}}(T - t_n),$$

and applying Taylor's theory

$$\begin{aligned}\max_{\overline{\Omega}}\{u(x, t_{n+1})\} - \max_{\overline{\Omega}}\{u(x, t_n)\} &\approx \left[(T - t_n) - \frac{\mathrm{d}t}{[\max_{\overline{\Omega}}\{u(x, t_n)\}]^{\kappa}}(T - t_n)\right]^{-2\beta} - (T - t_n)^{-2\beta}\\ &\approx 2\beta\frac{\mathrm{d}t}{[\max_{\overline{\Omega}}\{u(x, t_n)\}]^{\kappa}}(T - t_n)^{-2\beta}\\ &\approx 2\beta\mathrm{d}t(T - t_n)^{-2\beta(1-\kappa)}.\end{aligned}$$

In the critical case $\kappa = 1$, we have

$$\max_{\overline{\Omega}}\{u(x, t_{n+1})\} - \max_{\overline{\Omega}}\{u(x, t_n)\} \approx 2\beta\mathrm{d}t.$$

Then $\max_{\overline{\Omega}}\{u(x, t)\}$ is increased by nearly a constant size as the time evolves. Meanwhile, for the other critical case $\kappa = 0$, the peak value of the solution is increased proportionally to the blowup rate $O((T-t)^{-2\beta})$. For small negative κ, i.e., $\gamma' < \frac{1}{2\beta}$, the solution value increases too fast to capture the blowup profile, while for large $\kappa > 1$, i.e., $\gamma' > \frac{1}{2\beta} + 1$, the time step is too small and thus the integration is too slow. Therefore, the practical value of γ' should be between $\frac{1}{2\beta}$ and $\frac{1}{2\beta} + 1$. In fact our experiment shows that for the choice $\gamma' < \frac{1}{2\beta}$ the program ceases running before reaching the blowup peak.

We summarize the numerical results for (7) with $p = 2$ and $p = 4$ in Table 2, for (13) with $\{p = 3, q = 1\}$ and $\{p = 3, q = 2\}$ in Table 3, and for (16) with $\{p = 1, q = 1\}$, $\{p = 1, q = 2\}$, $\{p = 2, q = 1\}$ in Table 4. The blowup time

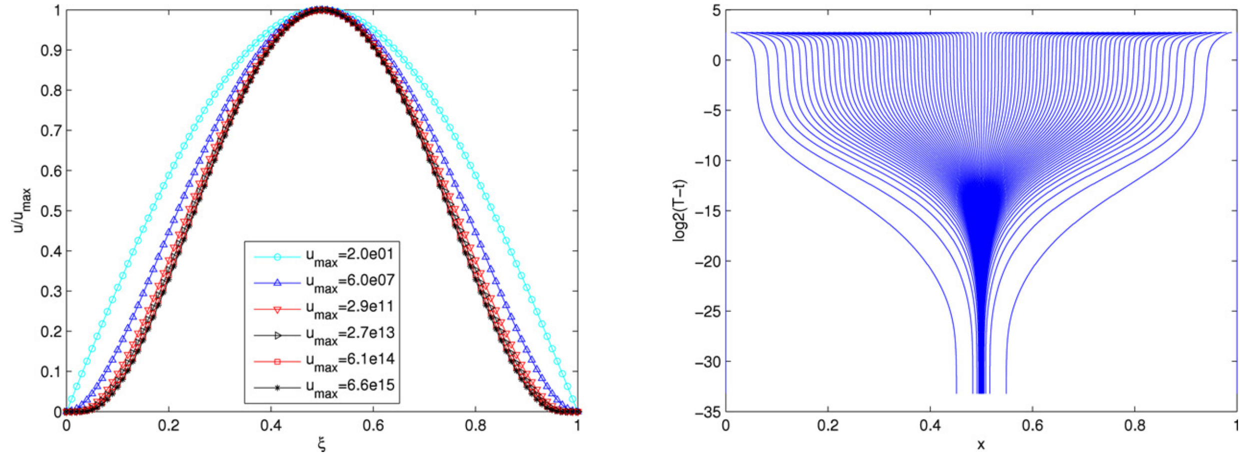

Fig. 1. Figs. for (7) with $p = 2$.

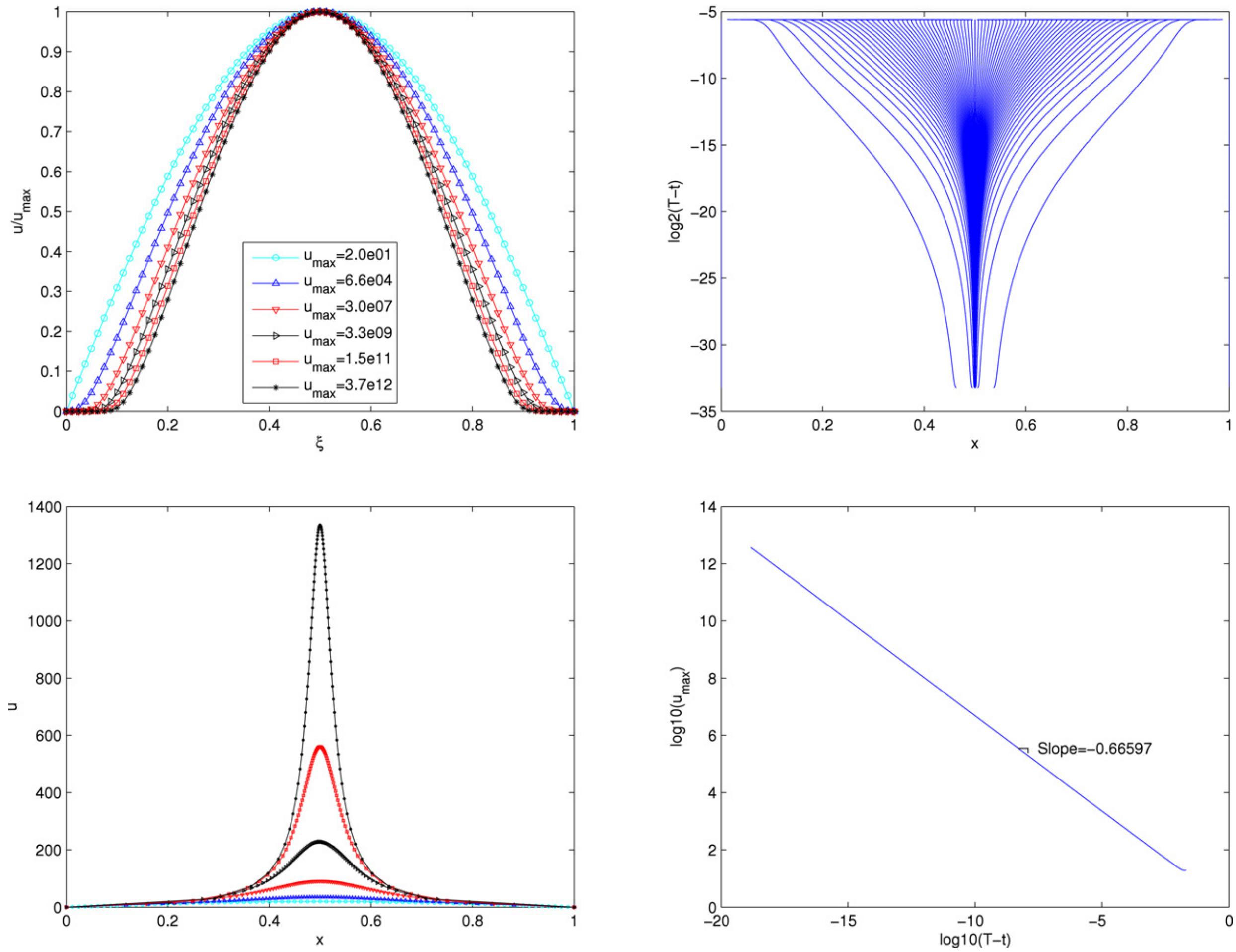

Fig. 2. Figs. for (7) with $p = 4$.

Table 2
Summary of numerical results for (7).

p	$\gamma, \tau, \gamma', \mathrm{d}t$	Blowup time	Blowup rate $(T-t)^{-\sigma}$	Figures
2	0.7, 1, 0.6, 0.5	6.703495010970e0	$\sigma = 1.9940$	Fig. 1
4	1.5, 1e-3, 1.505, 1e-2	2.062736979605e-2	$\sigma = 0.6660$	Fig. 2

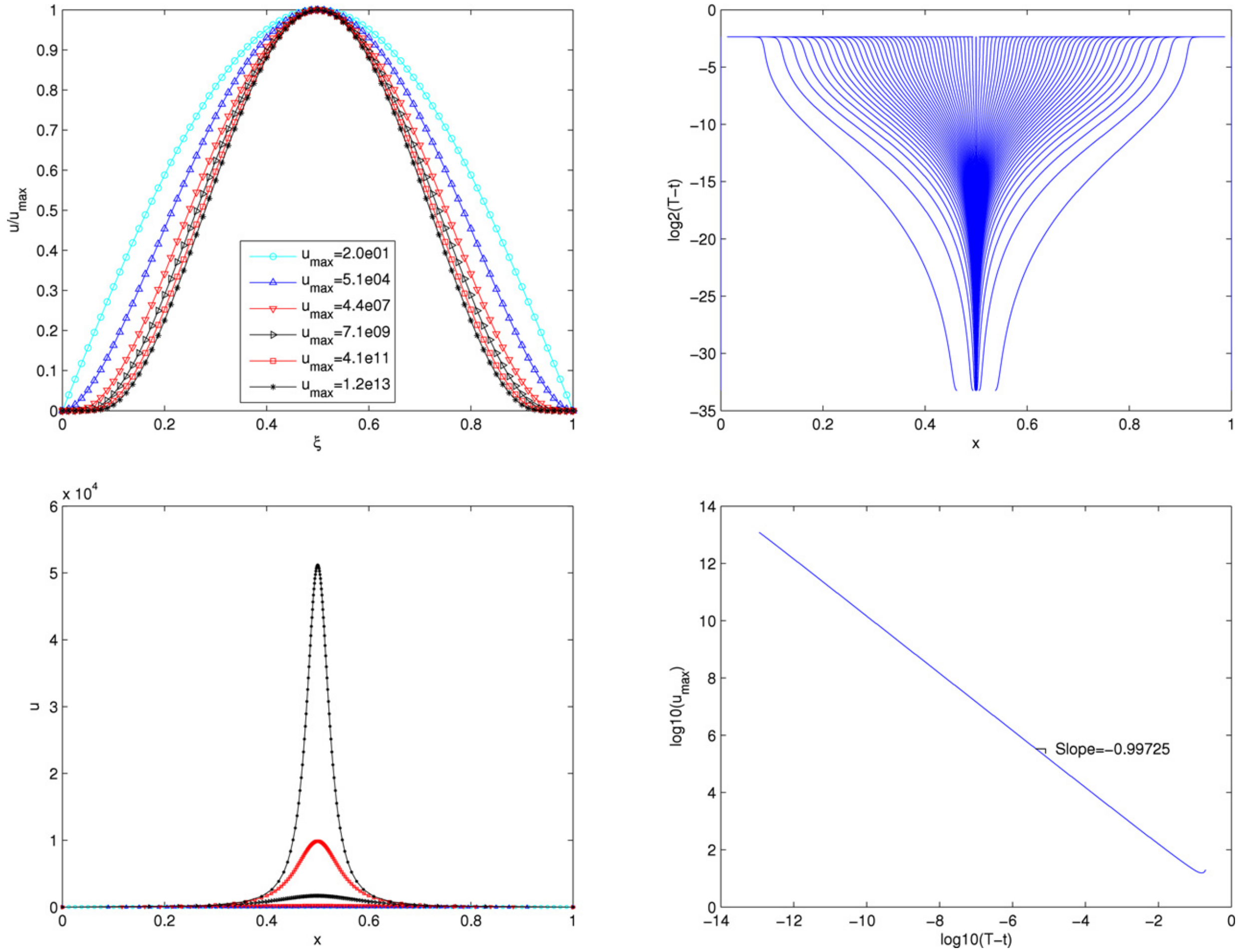

Fig. 3. Figs. for (13) with $p = 3$, $q = 1$.

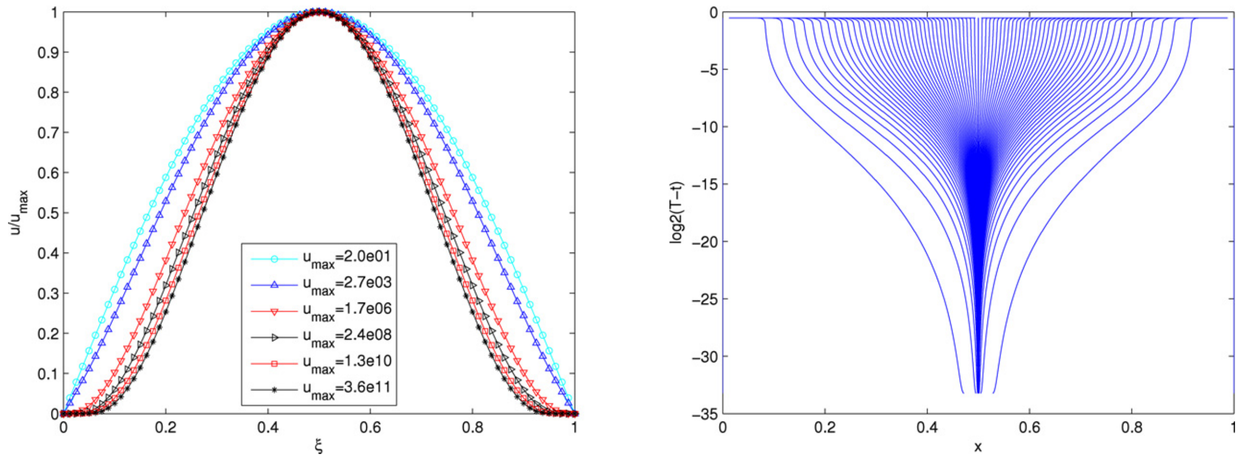

Fig. 4. Figs. for (13) with $p = 3$, $q = 2$.

Table 3
Summary of numerical results for (13).

p, q	$\gamma, \tau, \gamma', \mathrm{d}t$	Blowup time	Blowup rate $(T - t)^{-\sigma}$	Figures
3, 1	1, 1e-3, 1.05, 1e-2	1.959739831932e-1	$\sigma = 0.9973$	Fig. 3
3, 2	1, 1e-3, 1.05, 1e-2	6.897727699391e-1	$\sigma = 0.9950$	Fig. 4

Table 4
Summary of numerical results for (16).

p, q	$\gamma, \tau, \gamma', \mathrm{d}t$	Blowup time	Blowup rate $(T-t)^{-\sigma}$	Figures
1, 1	0.7, 1, 0.6, 5e-2	5.437117205300e-1	$\sigma = 1.9974$	Fig. 5
1, 2	1.2, 1e-2, 1.2, 5e-2	1.414864946512e-2	$\sigma = 0.9765$	Fig. 6
2, 1	1.2, 1e-3, 1.2, 5e-2	2.036640861114e-2	$\sigma = 0.9986$	Fig. 7

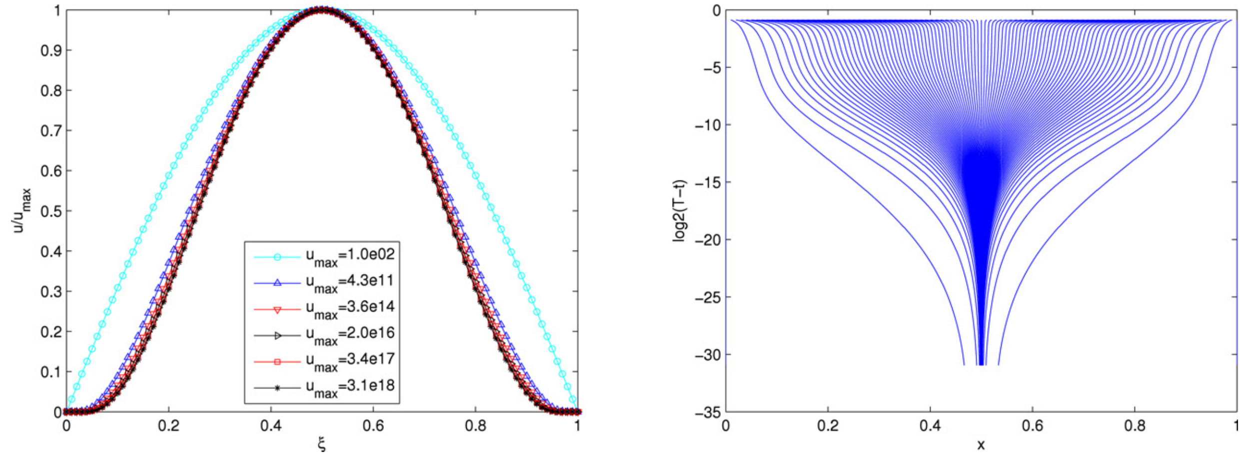

Fig. 5. Figs. for (16) with $p = 1, q = 1$.

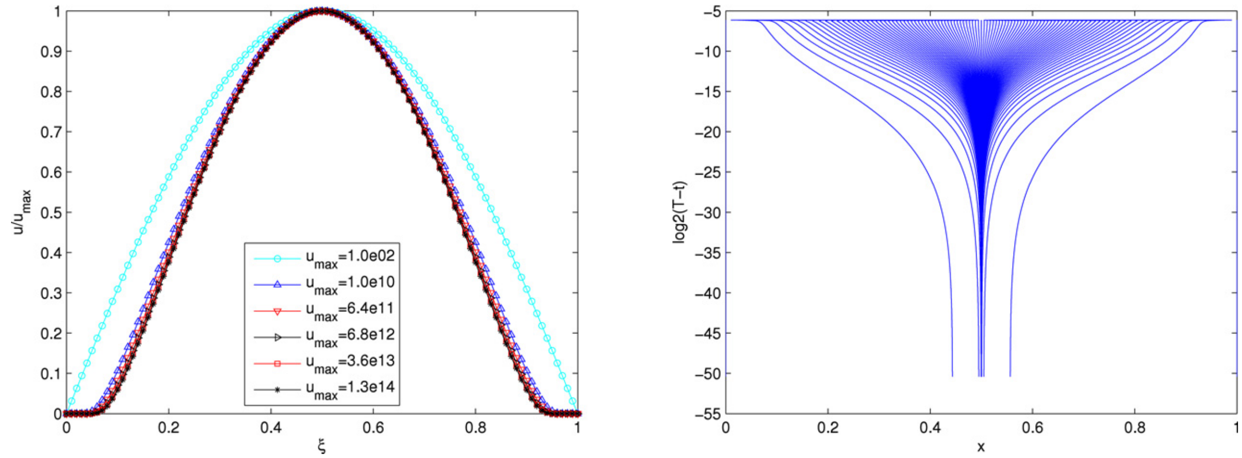

Fig. 6. Figs. for (16) with $p = 1, q = 2$.

is approximately the termination time using a large number of spatial mesh points and integrating for a long time till the maximum value of solution attains around 10^{15}. Usually the blowup rate has the form

$$u_{\max} \approx (T-t)^{-\sigma}.$$

Therefore, the value of σ can be given by

$$\sigma = \left| \frac{\log 10(u_{\max})}{\log 10(T-t)} \right|.$$

The constant τ in MMPDE6 is given by a value between 10^{-3} and 1, the parameter γ' in the time-step formula (20) is adjusted accordingly from $\frac{p-1}{2}$ to $\frac{p-1}{2}+1$ for (7) and (13), and from $\frac{p+q-1}{2}$ to $\frac{p+q-1}{2}+1$ for (16). The monitor function is taken as the form $M = u^{\gamma}$ with γ determined by Table 1.

The figures on ξ v.s. $u/u_{\max}$ show that the blowup profiles can be represented by functions of ξ. The figures on mesh trajectories indicate that the mesh evolves properly in accordance with the blowup motion. The figures on x v.s. u elucidate that the physical solutions have self-similar properties. The slopes of the lines $-\log 10(T-t)$ v.s. $\log 10(u/u_{\max})$ give the blowup rates.

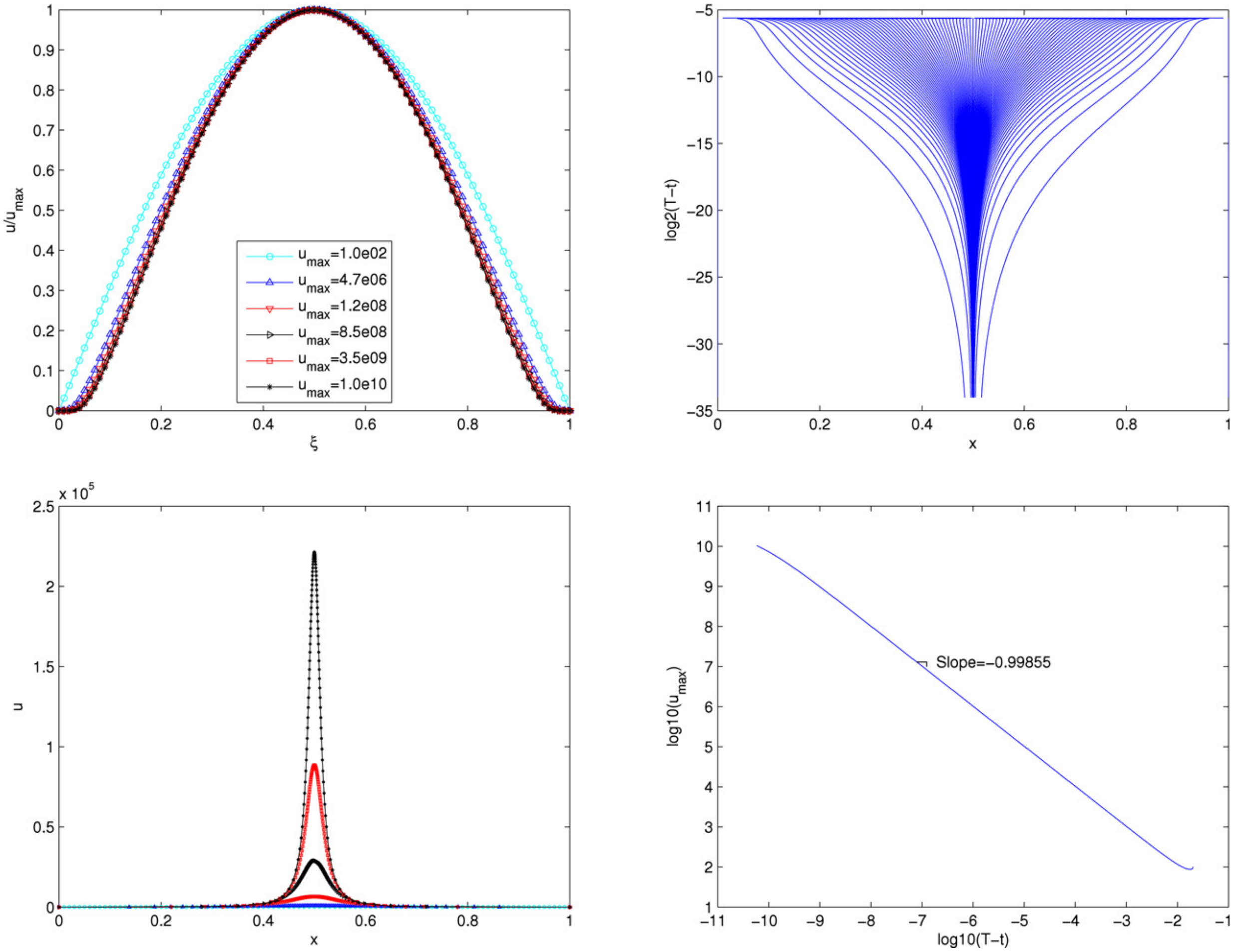

Fig. 7. Figs. for (16) with $p = 2, q = 1$.

3. Problems with nonlocal reaction terms in space

3.1. Dimensional analysis and monitor functions

We consider the equation

$$u_t - u_{xx} = u^p - \int_{\Omega} u^q(y, t)\, \mathrm{d}y, \quad t > 0, x \in \Omega \subset \mathbb{R}, \tag{21}$$

with $u|_{\partial\Omega} = 0$, $u(x, 0) = u_0(x)$. It is proved by [27] (compare also [29]) that if $p > q \geq 1$ for sufficiently large initial data, the solution has finite time blowup with the rate

$$\max_{x\in\overline{\Omega}} |u(x, t)| \approx (T - t)^{-1/(p-1)}, \quad \text{as } t \to T.$$

Moreover if $p = q > 1$, for sufficiently large initial data, the solution blows up with the same rate (see cf. [29,28]). Paper [6] gives a proof for $p = q = 2$ with an integral constraint.

Let $v + w = u$. Then we can split Eq. (21) into two equations:

$$v_t - v_{xx} = u^p; \tag{22}$$

$$w_t - w_{xx} = -\int_{\Omega} u^q(x, s)\, \mathrm{d}s. \tag{23}$$

Note that $[v] = [w] = [u]$. Then for (22) and (23), the dimensional equations are, respectively,

$$\frac{[u]}{[t]} = \frac{[u]}{[x]^2} = [u]^p,$$

Table 5
Monitor functions $M = u^\gamma$ for Eq. (21) and $M = (\exp(u))^\gamma$ for Eq. (24).

Eq. (21) with $p > q \geq 1$	Eq. (24) with $0 < p < 1$
$\gamma \geq \max\{p-1, q-1\}$	$\gamma \geq \frac{1-p}{1+\sigma}$

Table 6
Summary of numerical results for (21).

p, q	$\gamma, \tau, \gamma', \mathrm{d}t$	Blowup time	Blowup rate $(T-t)^{-\sigma}$	Figures
2, 1	1.2, 1e-2, 1.25, 5e-2	9.016158665247e-2	$\sigma = 0.9979$	Fig. 8
3, 2	2.0, 1e-4, 2.2, 1e-2	2.052723443594e-3	$\sigma = 0.4999$	Fig. 9

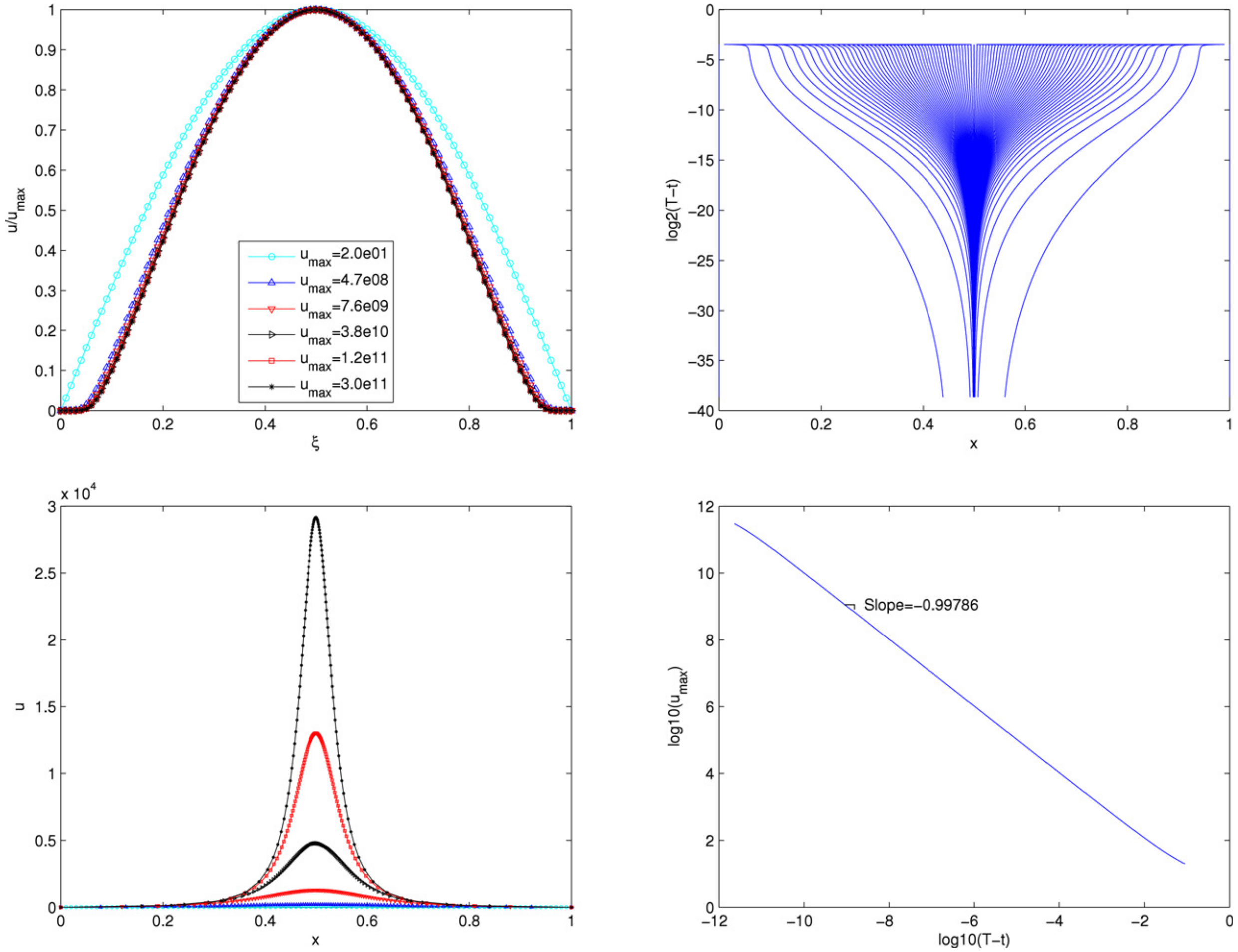

Fig. 8. Figs. for (21) with $p = 2, q = 1$.

and

$$\frac{[u]}{[t]} = \frac{[u]}{[x]^2} = [u]^q.$$

Therefore, combining the dimensional Eq. (11) for MMPDE6 we obtain a sufficient condition for dominance of equidistribution, $\beta\gamma \geq 1$ and $\eta\gamma \geq 1, \eta = 1/(q-1)$ (when equalities hold, τ has to be sufficiently small to keep the dominance of equidistribution). Hence for Eq. (21), it requires that $\gamma \geq \max\{1/\beta, 1/\eta\}$ to keep the dominance of equidistribution.

In addition, we study equation of the form, see e.g., [2],

$$u_t - u_{xx} = \frac{\exp(u)}{\left(\int_\Omega \exp(u(y,t))\,\mathrm{d}y\right)^p}, \quad 0 < p < 1, t > 0, x \in \Omega \subset \mathbb{R}, \tag{24}$$

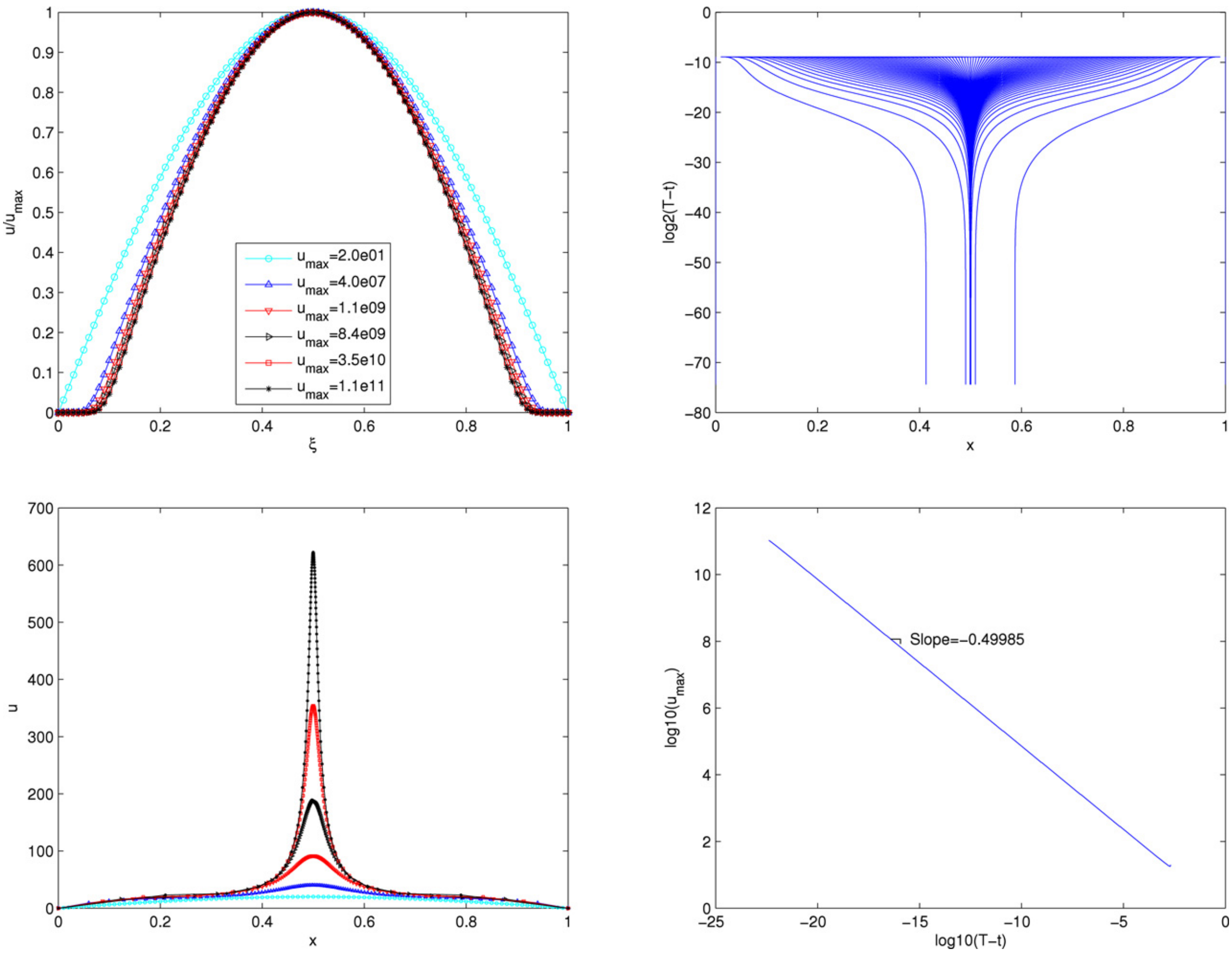

Fig. 9. Figs. for (21) with $p = 3, q = 2$.

Table 7
Summary of numerical results for (24).

p	$\gamma, \tau, \gamma', \mathrm{d}t$	Blowup time	Blowup rate $\mathrm{e}^{u_{\max}} = (T - t)^{-\sigma}$	Figures
0.2	1, 0.1, 1.2, 0.5	3.027592917836e-4	$\sigma = 1.1216$	Fig. 10
0.5	1, 0.1, 1, 1	1.945134299942e-2	$\sigma = 1.4745$	Fig. 11

with $u|_{\partial\Omega} = 0$, $u(x, 0) = u_0(x)$.

The dimensional analysis gives that

$$\frac{[u]}{[t]} = \frac{[u]}{[x]^2} = \frac{[\exp(u)]}{[\exp(u)]^p},$$

which derives that

$$[u][\exp(u)]^{p-1} = [t]. \tag{25}$$

Use monitor function of the form $M = (\exp(u))^\gamma$. Then (10) gives that

$$\frac{[\tau]}{[t][\exp(u)]^\gamma} = 1. \tag{26}$$

Combining (25) with (26) and assuming that

$$\max_{x\in\overline{\Omega}} u(x, t) \approx (T - t)^{-\sigma}, \quad \text{as } t \to T, \sigma > 0,$$

we obtain that

$$[\tau][T - t]^{\frac{-\gamma(\sigma+1)-(p-1)}{p-1}} = 1. \tag{27}$$

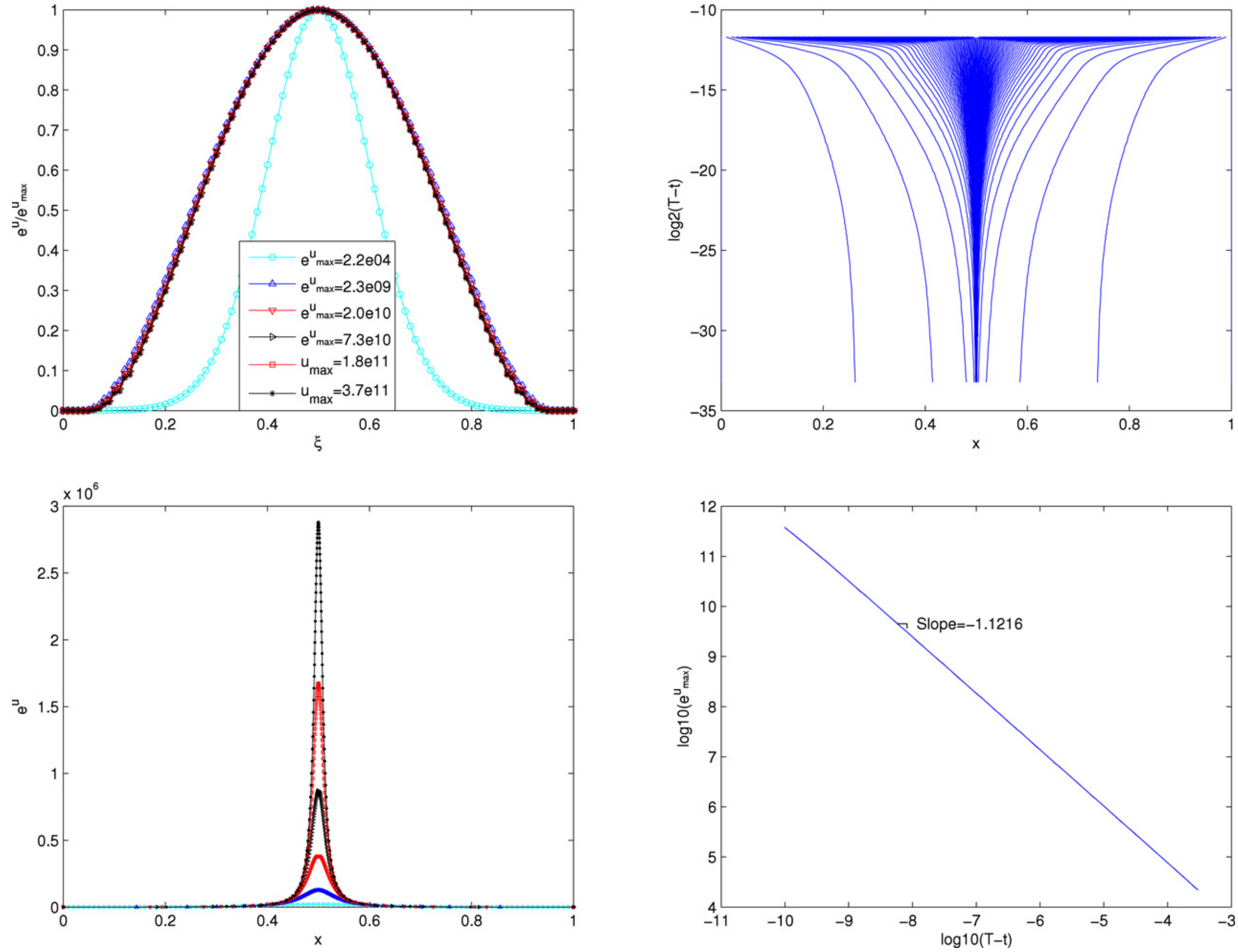

Fig. 10. Figs. for (24) with $p = 0.2$.

Hence it requires that

$$\gamma \geq \frac{1-p}{\sigma+1}$$

to guarantee the dominance of equidistribution.

We summarize the results of this section in Table 5.

3.2. Numerical experiments

Let $\Omega = (0, 1)$ and take $N = 101$. We give the numerical results for problem (21) with initial condition $u_0 = 20\sin(\pi x)$, and (24) with $u_0 = 10\sin(\pi x)$.

The solution process is given in Algorithm 1 with replacements of f terms in (17) and (19), respectively, by

$$f\left(\widetilde{u}_j^{n+1}, \sum_{j=1}^{N}(x_{j+1}^n - x_j^n)\frac{g(t_{n+1}, \widetilde{u}_j^{n+1}) + g(t_{n+1}, \widetilde{u}_{j+1}^{n+1})}{2}\right)$$

and

$$f\left(u_j^{n+1}, \sum_{j=1}^{N}(x_{j+1}^{n+1} - x_j^{n+1})\frac{g(t_{n+1}, u_j^{n+1}) + g(t_{n+1}, u_{j+1}^{n+1})}{2}\right).$$

For (21), the monitor function is given by $M = u^\gamma$, where γ is given in Table 5. The numerical results which are summarized in Table 6 are consistent with our desired results.

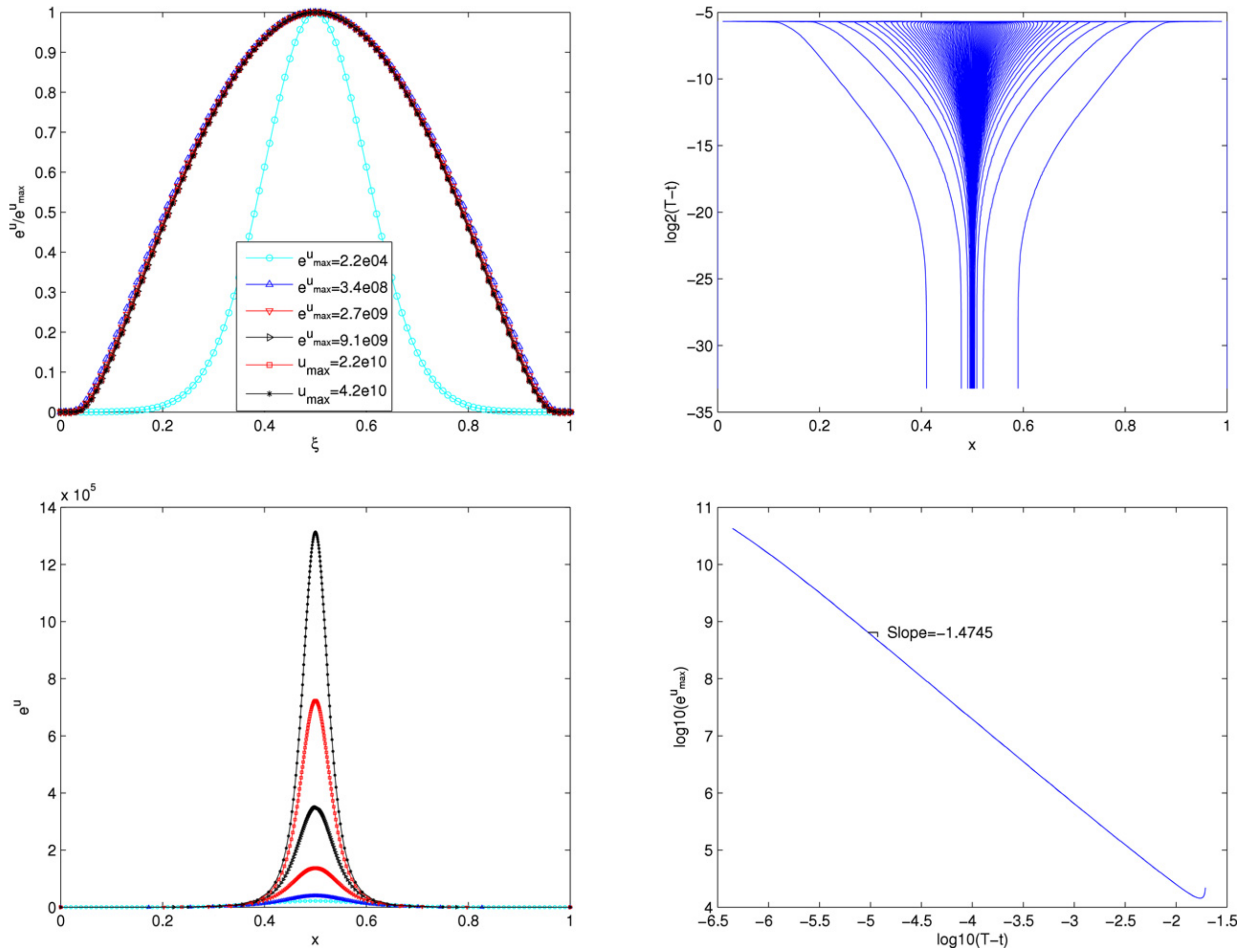

Fig. 11. Figs. for (24) with $p = 0.5$.

For problem (24), the integration time step is given by

$$\Delta t_n = \frac{\mathrm{d}t}{[\max\limits_{(j)} \exp(u_j^n)]^{\gamma'}}.$$

The monitor function is of the form

$$M = (\exp(u))^{\gamma},$$

where γ is determined by Table 5. The numerical results are given in Table 7 and the figures are listed in the table. The numerical results indicate that our MMPDE methods are efficient to resolve this type of blowup problems.

4. Conclusions

In this paper, we have implemented the moving mesh PDE methods to numerical simulation of the blowup in reaction–diffusion equations with nonlinear nonlocal terms in space and time. The physical equation and the MMPDE are solved alternately, unlike the traditional MMPDE methods (see e.g., [7,5,24,25,16]) solve the coupled system by an integration solver — DASSL (see [21]). The problems we investigate in this paper have finite time blowup solutions at fixed single point. Numerical results expose the self-similar properties in blowup solutions, though the general theory has not been found yet. The more complex space–time coupled nonlocal reaction–diffusion equations are not included in the present work. In most cases, such problems have global blowup solutions. Hence the gradient-based monitor functions should be used and a new dimensional analysis should be performed in this situation. The in-depth investigation will be carried out elsewhere.

Acknowledgements

J. Ma is grateful to Bob Russell for his support through a NSERC (Canada) Grant. The authors would also like to thank the anonymous referee for the constructive suggestions that lead to a greatly improved paper.

References

[1] J.W. Bebernes, P. Talaga, Nonlocal problems modelling shear banding, Comm. Appl. Nonlinear Anal. 3 (1996) 79–103.
[2] J.W. Bebernes, C. Li, P. Talaga, Single-point blowup for nonlocal parabolic problems, Physica D 134 (1999) 48–60.
[3] C. Bandle, H. Brunner, Blowup in diffusion equations: A survey, J. Comput. Appl. Math. 97 (1998) 3–22.
[4] G.I. Barenblatt, Scaling, Self-Similarity, and Intermediate Asymptotics, Cambridge University Press, 1996.
[5] C.J. Budd, R. Carretero-González, R.D. Russell, Precise computations of chemotactic collapse using moving mesh methods, J. Comput. Phys. 202 (2005) 463–487.
[6] C. Budd, B. Dold, A. Stewart, Blowup in a partial differential equation with conserved first integral, SIAM J. Appl. Math. 53 (1993) 718–742.
[7] C.J. Budd, W.Zh. Huang, R.D. Russell, Moving mesh methods for problems with blow-up, SIAM J. Sci. Comput. 17 (1996) 305–327.
[8] C. Chen, T. Shih, Finite Element Methods for Integro–Differential Equations, in: Series on Applied Math., vol. 9, World Scientific, Singapore, 1998.
[9] J.M. Cushing, Integro–Differential Equations and Delay Models in Population Dynamics, in: Lecture Notes Biomath., vol. 20, Springer-Verlag, New York, 1977.
[10] C. de Boor, Good approximation by splines with variable knots II, in: Springer Lecture Notes Series, vol. 363, Springer-Verlag, Berlin, 1973.
[11] W.H. Deng, Short memory principle and a predictor–corrector approach for fractional differential equations, J. Comput. Appl. Math. 206 (2007) 174–188.
[12] W.H. Deng, Numerical algorithm for the time fractional Fokker–Planck equation, J. Comput. Phys. 227 (2007) 1510–1522.
[13] M. Fila, Boundedness of global solutions of nonlocal parabolic equations, Nonlinear Anal. 30 (1997) 877–885.
[14] Y. Fujita, Integral equation which interpolates the heat equation and the wave equation, Osaka J. Math. 27 (1990) 309–321. 28 (1990), pp. 797–804.
[15] D. Hirata, Blow-up for a class of semilinear integro-differential equations of parabolic type, Math. Methods Appl. Sci. 22 (1999) 1087–1100.
[16] W.Zh. Huang, J. Ma, R.D. Russell, A study of moving mesh PDE methods for numerical simulation of blowup in reaction diffusion equations, J. Comput. Phys. 227 (2008) 6532–6552.
[17] W.Zh. Huang, Y. Ren, R.D. Russell, Moving mesh partial differential equations (MMPDEs) based upon the equidistribution principle, SIAM J. Numer. Anal. 31 (1994) 709–730.
[18] Y. Jiang, J. Ma, K. Xiang, A moving mesh method for partial integro–differential equation, J. Comput. Math. (2008) (submitted for publication).
[19] A. Khozanov, Parabolic equations with nonlocal nonlinear source, Siberian Math. J. 35 (1994) 545–556.
[20] Y. Li, C. Xie, Blow-up for semilinear parabolic equations with nonlinear memory, Z. Angew. Math. Phys. 55 (2004) 15–27.
[21] L.R. Petzold, A description of DASSL: A differential/algebraic system solver, Sandia Labs Report SAND82-8637, Livermore, CA, 1982.
[22] C.A. Roberts, Recent results on blow-up and quenching for nonlinear Volterra equations, J. Comput. Appl. Math. 205 (2007) 736–743.
[23] C.A. Roberts, W.E. Olmstead, Growth rates for blow-up solutions of nonlinear Volterra equations, Quart. Appl. Math. 54 (1996) 153–159.
[24] R.D. Russell, J.F. Williams, X. Xu, MOVCOL4: A moving mesh code for fourth-order time-dependent partial differential equations, SIAM J. Sci. Comput. 29 (2007) 197–220.
[25] A.R. Soheili, J.M. Stockie, A moving mesh method with variable mesh relaxation time, Appl. Numer. Math. 58 (2008) 249–263.
[26] P. Souplet, Blow-up in nonlocal reaction–diffusion equations, SIAM J. Math. Anal. 29 (1998) 1301–1334.
[27] P. Souplet, Uniform blow-up profiles and boundary behavior for diffusion equations with nonlocal nonlinear source, J. Differential Equation 153 (1999) 374–406.
[28] P. Souplet, Monotonicity of solutions and blow-up for semilinear parabolic equations with nonlinear memory, Z. Angew. Math. Phys. 55 (2004) 28–31.
[29] M. Wang, Y. Wang, Properties of positive solutions for non-local reaction–diffusion problems, Math. Methods Appl. Sci. 19 (1996) 1141–1156.